



Hydrogen absorption of Nb–Al alloy bulk specimens

Hideki Hosoda*, Tatsuo Tabaru, Satoshi Semboshi¹, Shuji Hanada

Institute for Materials Research, Tohoku University, 2-1-1 Katahira, Aoba-ku, Sendai 980-8577, Japan

Received 9 May 1998; received in revised form 6 July 1998

Abstract

Pulverization by hydrogenation is applicable to powder fabrication for refractory intermetallic alloys. Hydrogen absorption of various Nb–Al alloys containing 0–28 mol% Al was investigated using bulk specimens in a Sieverts-type apparatus at test temperatures of 313–373 K under hydrogen pressure of 0–3.4 MPa. The lattice parameter of Nb solid solution (Nb_{ss}) was determined precisely as a function of Al concentration. It was found that (1) the lattice parameter of Nb_{ss} is linearly reduced with increasing Al content, and (2) hydrogen absorption of Nb_{ss} is also remarkably reduced by Al addition. The atomic radius of Al in Nb_{ss} is determined to be 139.2 pm. Large hydrogen absorption more than 0.5 mass% H is observed only for pure Nb and Nb_3Al -based two-phase alloys. However, pulverization and the large hydrogen absorption at a constant pressure (plateau) take place only in the latter alloys. This plateau does not stand for equilibrium hydride formation, but for rapid absorption through increased surface area by pulverization. These aspects are discussed in connection with hydrogen diffusivity. © 1998 Elsevier Science S.A. All rights reserved.

1. Introduction

Nb_3Al intermetallic alloys have been expected to be ultra-high temperature structural materials due to a high melting point and superior specific strength [1–3]. The improvement of room-temperature ductility and toughness, however, has still not been overcome for Nb_3Al alloys. It is generally accepted that one of the most promising methods for toughness improvement of brittle materials is to distribute a ductile second phase in a brittle phase. In the Nb_3Al -based alloys, a niobium solid solution (Nb_{ss}) having a disordered bcc crystal structure (A2) may behave as a ductile phase in a brittle Nb_3Al (A15) phase. In addition, since these two-phase alloys are thermally stable at elevated temperatures, as shown in the Nb–Al binary phase diagram [4–6], the combination should show a high potential as an ultra-high temperature structural material.

In producing and forming Nb_3Al/Nb_{ss} two-phase alloys, a powder metallurgy process is advantageous, although powder preparation is costly in using conventional powder fabrication methods. Recently, we have investigated hydrogenation of Nb_3Al -based alloys around ambient temperatures, and it was found that (1) only two-phase alloys

(Nb_{ss}/Nb_3Al and Nb_3Al/Nb_2Al) are pulverized, and (2) Nb_{ss}/Nb_3Al two-phase alloys absorb a large amount of hydrogen under a constant hydrogen pressure (so-called plateau) when pulverized [6,7]. It should be mentioned that no hydride formation is recognized in any case. In this paper, a ‘hydride’ stands for a compound, the crystal structure of which is different from that of the mother alloy. An alloy (or compound) dissolving hydrogen is not recognized to be a ‘hydride’ if the crystal structure is not changed through hydrogen absorption. Moreover, a large volume change of Nb_{ss} due to hydrogen absorption was shown to play an important role in pulverization. The results of X-ray diffractometry suggest that the pulverization of the Nb–Al alloys is caused by the strain energy generated between different phases through hydrogenation [7]: Nb_3Al is brittle at ambient temperature and it is fractured even in two-phase alloys containing ductile Nb_{ss} . For developing the hydrogen pulverization as a new powder fabrication method for Nb–Al alloys, a further understanding of hydrogen absorption of various Nb–Al alloys is required. The object of this study is to clarify the characteristics of hydrogen absorption of single phase alloys (Nb, Nb_{ss} and Nb_3Al) and two-phase alloys (Nb_{ss}/Nb_3Al and Nb_3Al/Nb_2Al) using relatively large bulk specimens. In addition, the lattice parameter of Nb_{ss} is determined as a function of Al content: the lattice parameter is important for pulverization by hydrogenation as well

*Corresponding author.

¹ Graduate student, Tohoku University, 2-1-1 Katahira, Aoba-ku, Sendai 980-8577, Japan.

as alloy designing in high temperature structural materials. These characters are discussed in connection with hydrogen diffusivity and lattice expansion by hydrogen absorption.

2. Experimental procedure

Based on the Nb–Al phase diagram in Fig. 1 Ref. [4], three kinds of single phase alloys of Nb (pure Nb), Nb–3.0% Al (Nb_{ss}) and Nb–21.1% Al (Nb_3Al), and three kinds of two-phase alloys of Nb–16.2% Al and Nb–18.1% Al ($\text{Nb}_{\text{ss}}/\text{Nb}_3\text{Al}$) and Nb–28.1% Al ($\text{Nb}_3\text{Al}/\text{Nb}_2\text{Al}$) were prepared for measuring hydrogen absorption. All compositions are given in mole percent by inductively coupled plasma (ICP) emission spectrochemical analysis. These alloys will be abbreviated hereafter as Nb–3Al, Nb–21Al, Nb–16Al, Nb–18Al and Nb–28Al. They were Ar arc-melted using starting materials of 99.97%Nb and 99.99%Al. Homogenization was carried out in vacuum at 2073 K for 10.8 ks for Nb–28Al, and at 2173 K for 10.8 ks for the others. And they were heat-treated at 1473 K for 86.4 ks in vacuum. The microstructures of these alloys were reported previously [6,7]. For supplying to electron probe microanalysis (EPMA), Nb_{ss} particles in $\text{Nb}_{\text{ss}}/\text{Nb}_3\text{Al}$ two-phase alloys after the above treatments appear to be too small to be analyzed. Thus, a combination of thermo-mechanical treatments was used to obtain coarse Nb_{ss} particles for EPMA. The details are as follows: Homogenization was carried out at 2173 K for 3.6 ks in vacuum. Isothermal forging was performed at 1473 K in vacuum for Nb–16Al and 1873 K for Nb–18Al: final reductions were near 75% in thickness with a nominal strain rate of $3 \times 10^{-5} \text{ s}^{-1}$. Then, the alloys were heat-treated at 1473 K for 612 ks in vacuum, and alloys were furnace cooled (less than 10 min to 1000 K in all tests). Equiaxed crystal grains, which are large enough in size for EPMA, were formed by the combination of the heat treatments and isothermal forging. EPMA was performed

more than ten times using the electropolished alloys. Employed compositions were averaged. For the lattice parameter measurements, XRD analysis of conventional θ – 2θ scan was carried out at room temperature where the angle scanned was from 20° to 140° in 2θ . $\text{CuK}\alpha$ by Cu-tube (40 mA, 40 kV) and β -filter of Ni plate were used and a scan step was chosen to be 0.025° in 2θ . Precise lattice parameters were determined by extrapolating lattice parameters measured as a function of $\cos^2\theta$. For measuring hydrogen absorption, rectangular bulk specimens of $4.5 \times 4.5 \times 2$ mm were made by an electro-discharge machine. The surfaces of specimens were mechanically polished in Ar to obtain a fresh surface. Without exposure to air, hydrogen absorption followed by desorption was measured at 313–373 K under the hydrogen pressure of 0–3.4 MPa using a conventional Sieverts-type apparatus produced by LESCA. In this automatic measurement system, hydrogen pressure was variable and a hydrogen content under a hydrogen pressure was determined to be at ‘equilibrium’ when deviations from a set pressure were less than 0.001 MPa during 25 data points. It took about 4 h to obtain every hydrogen absorption and desorption curve in this study: in many cases, it took longer in absorption measurements than in desorption measurements depending on the number of data points acquired. Hydrogen used was of high purity of 99.99999%. It should be noted that, even though the equilibrium pressure–composition–isotherms cannot be obtained due to such large specimens at these relatively low temperatures and due to hydrogen diffusion in Nb being sensitive to surface conditions [8], the hydrogen absorption curves obtained are believed to be an important indication for developing the powder-producing method based on hydrogen pulverization.

3. Results and discussion

3.1. Hydrogen absorption of single phase alloys

Fig. 2 shows hydrogen absorption and desorption curves of pure Nb (Nb), Nb_{ss} (Nb–3Al) and Nb_3Al (Nb–21Al) at 353 and 373 K. After hydrogenation, Nb maintains a large amount of hydrogen: 0.81 mass% H at 353 K and 0.75 mass% H at 373 K. No pulverization occurs in these single phase alloys with different Al contents regardless of the considerable amount of hydrogen absorption at the test temperatures. According to the Nb–H phase diagram shown in Fig. 3, these hydrogen contents (0.75 and 0.81 mass% H) are related to β -NbH hydride formation, the crystal structure of which is $\text{o}P8$ [9]. XRD patterns from the hydrogenized specimens show NbH-related or bcc-distorted pattern for pure Nb, and bcc pattern with a very small lattice expansion (less than 0.1%) for Nb–3Al. Hydride formation for pure Nb could not be confirmed from the result of XRD. This suggests that

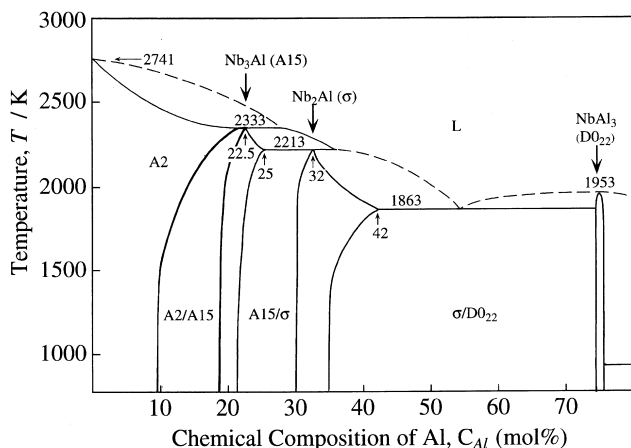


Fig. 1. The Nb–Al phase diagram reported by Jorda et al. [4].

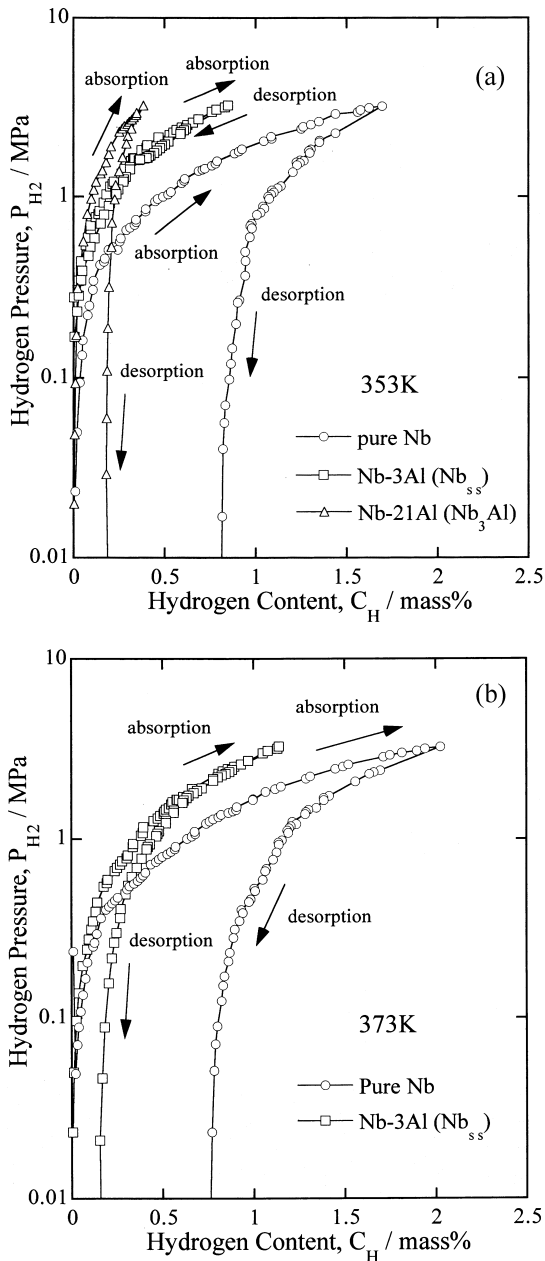


Fig. 2. Hydrogen absorption and desorption curves of pure Nb, Nb-3Al (Nb_{ss}) and Nb-21Al (Nb_3Al) single phase alloys: (a) 353 K and (b) 373 K.

peaks from the hydrogen sublattice were difficult to detect if ordered.

When a hydride is formed through hydrogen absorption, a ‘plateau’ is generally seen in the hydrogen absorption curves in hydrogen storage metals. The plateau usually stands for an equilibrium hydride formation in which a large amount of hydrogen absorption occurs under a constant hydrogen pressure. However, the plateau in the hydrogen absorption curve was not observed for pure Nb in this study even if β -NbH was formed. Fig. 4 shows the well-established hydrogen solubility curves for Nb in equilibrium state [10], in which plateaus are seen at

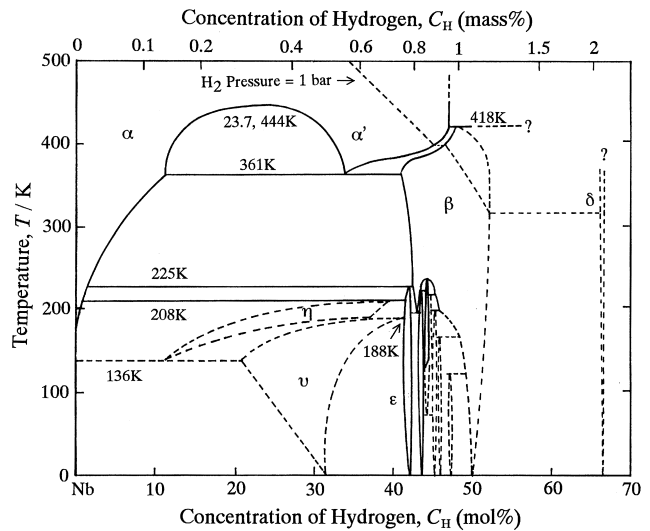


Fig. 3. The Nb-H phase diagram [9].

temperatures below 503 K. By comparing Fig. 2 with Fig. 4, it is obvious that the hydrogen absorption curves obtained in this study are not at equilibrium. Since the specimen size is relatively large ($4.5 \times 4.5 \times 2$ mm) in this study, hydrogen diffusivity around 10^{-9} m²/s at 350 K in Nb [8] may lead to the gradual formation of a hydride depending on hydrogen diffusion from the surface. If this is the case, the hydrogen absorption curves do not show the ‘plateau’ even in the gradual hydride formation. This suggests that hydride formation is not absolutely required for pulverization by hydrogenation, even though hydride formation may accelerate the pulverization if it happens.

By comparing Nb and Nb-3Al, it is clear that hydrogen absorption is much reduced by adding Al: hydrogen

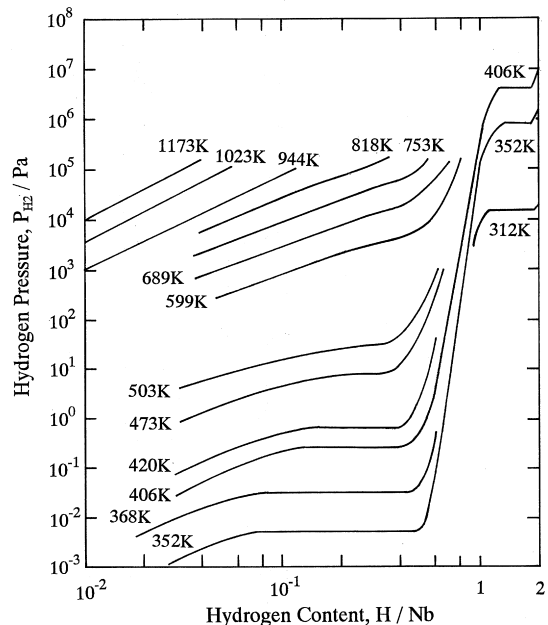


Fig. 4. Hydrogen solubility curves for niobium [10].

contents at 373 K are 0.75 mass% H in Nb and 0.15 mass% H in Nb–3Al after hydrogenation. This reduction of hydrogen absorption might be related to hydrogen diffusivity, which will be discussed in Section 3.5. Nb–21Al shows lower hydrogen content at 3.4 MPa but higher after relieving pressure than Nb–3Al. It is considered in Nb₃Al that the amount of hydrogen absorbed from the surface is small but hydrogen atoms tend to stay within the alloy probably because of low hydrogen diffusivity in the complex structure of A15.

3.2. Hydrogen absorption of Nb₃Al alloys

Fig. 5 shows the hydrogen absorption and desorption curves at 313 K and 353 K for the Nb₃Al-based alloys (Nb₃Al single phase, Nb_{ss}/Nb₃Al and Nb₃Al/Nb₂Al two-phase alloys). At 353 K, both two-phase alloys are pulverized by hydrogenation regardless of different constituent phases. At 313 K, however, only the Nb–28Al alloy consisting of Nb₃Al and Nb₂Al is pulverized under the test conditions. At either test temperature, Nb–21Al alloy consisting of a Nb₃Al single phase is not pulverized under the test conditions. The pulverization occurs when the ‘plateau’ appears on the hydrogen absorption curve, although no hydrides are recognized by X-ray diffraction analysis under the same experimental conditions (crystal structures of the alloys are not changed through hydrogenation) [7]. Thus, it is concluded that pulverization by hydrogenation is not related to hydride formation in Nb–Al alloys. The plateau in this case corresponds to the rapid absorption of hydrogen from the fresh surface formed by pulverization.

When pulverization occurs at 353 K, the amount of hydrogen absorption of Nb–28Al (Nb₃Al/Nb₂Al) is about twice as much as that of Nb–16Al (Nb_{ss}/Nb₃Al) after hydrogenation as shown in Fig. 5 (b). This difference in stored hydrogen content may be explained by the fact that Nb₂Al possesses a lot of interstitial sites due to the more complex crystal structure of D8_b than A2 (Nb_{ss}) or A15 (Nb₃Al). The number of interstitial sites may also explain the difference in hydrogen absorption just before pulverization: hydrogen absorption of Nb–16Al is 0.35 mass% H which is smaller than that of Nb–28Al (0.85 mass% H) at 353 K.

3.3. Pulverization by hydrogenation

Although the fracture toughness of Nb₃Al-based alloys is improved by introducing ductile Nb_{ss} [11], Nb₃Al particles are still brittle at ambient temperature. When absorbing hydrogen, internal stress is generated in two-phase alloys if the lattice expansions of constituent phases are different. The internal stress is proportional to the difference in lattice expansions and Young’s modulus (E), similar to thermal stress. When Nb–16Al alloy absorbs hydrogen at 353 K, the internal stress generated for Nb₃Al

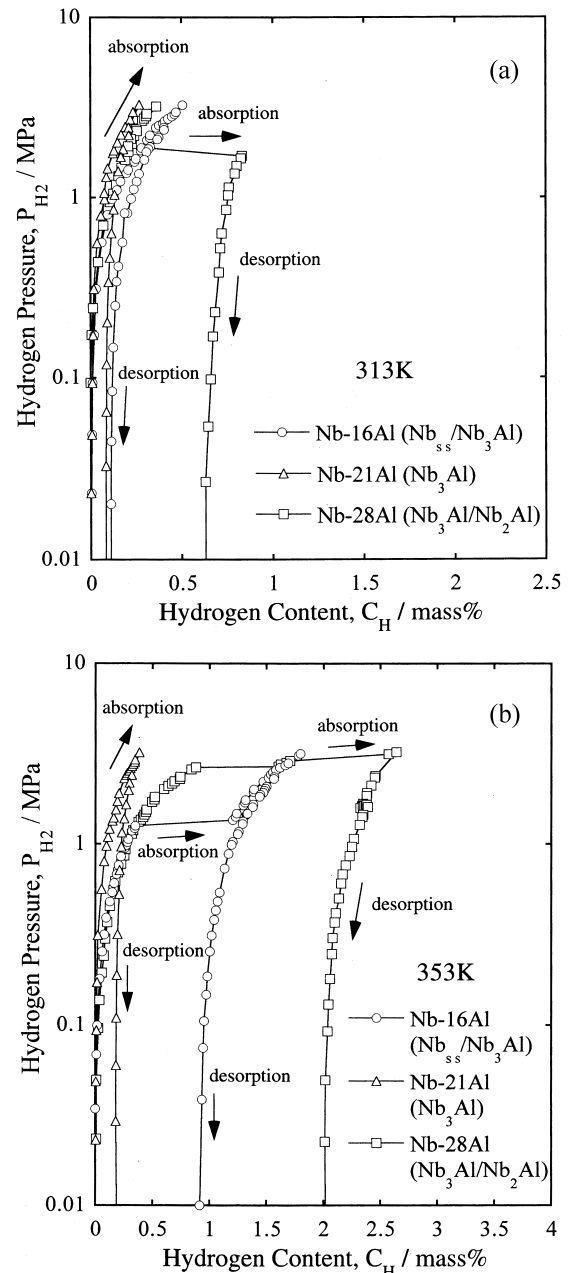


Fig. 5. Hydrogen absorption and desorption curves of Nb–16Al (Nb_{ss}/Nb₃Al), Nb–21Al (Nb₃Al) and Nb–28Al (Nb₃Al/Nb₂Al): (a) 313 K and (b) 353 K.

particles is estimated to be about 1.1 GPa using $E=135$ GPa [11] and the difference in lattice expansions between Nb_{ss} and Nb₃Al (0.8% [7]). This is much higher than fracture strength (272 MPa in flexure strength [11]). Therefore, pulverization occurs to release the strain energy in the two-phase alloys studied. The pulverization of Nb–28Al alloy can be explained similarly.

Consider the hydrogenation of the Nb₃Al single-phase alloys, and assume a gas diffusion in a semi-infinite system, the hydrogen pressure of 3.4 MPa (the maximum pressure used in this study), E of 135 GPa and no hydride

Table 1

Chemical compositions, constituent phases and Al concentration of Nb solid solution (Nb_{ss}) of the alloys investigated

Alloys	Chemical compositions	Equilibrated temperature	Constituent phases	Al concentration of Nb_{ss} (mol%)
Nb	99.97 mol% Nb	2173 K	Nb (A2)	0
Nb–3Al	Nb–3.0 mol% Al	2173 K	Nb_{ss} (A2)	3.0 (by ICP)
Nb–16Al	Nb–16.2 mol% Al	1473 K	Nb_{ss}/Nb_3Al	5.0 (by EPMA)
Nb–18Al	Nb–18.1 mol% Al	1873 K	Nb_{ss}/Nb_3Al	10.8 (by EPMA)

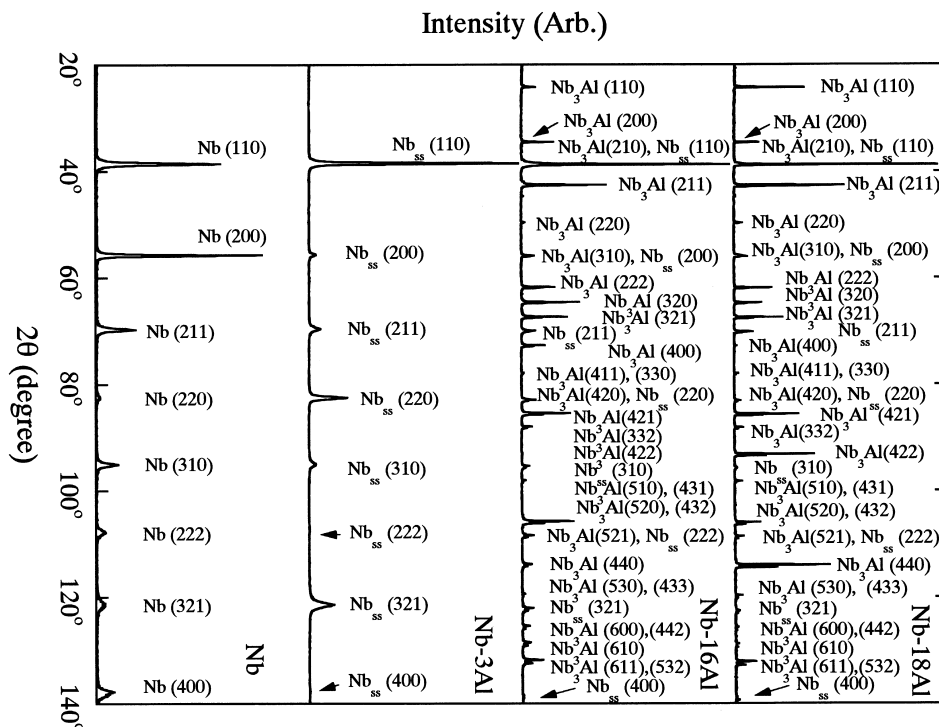
formation. Even in this case, the internal stress is still generated due to the hydrogen-concentration gradient. The maximum internal stress with the highest gradient is estimated to be about 8 MPa for Nb_3Al [12]. The value is much lower than the fracture stress. No other internal stress (for instance, due to the difference in lattice expansions) is generated. Thus, Nb–21Al was not pulverized even though Nb_3Al is brittle at ambient temperature.

3.4. Lattice parameter

It was revealed that hydrogen pulverization in Nb–Al alloys is caused due to the lattice volume expansion through hydrogenation, especially the difference in the expansions between constituent phases [6,7]. Then, the lattice parameter is an important factor for this powder producing method, as well as alloy design of high-temperature structural materials (degree of lattice mismatch is dominant for growth of precipitates and creep resistance

[13]). The lattice parameters of Nb_3Al and Nb_2Al were already investigated, and that of Nb_3Al is almost constant independently of alloy composition [7]. On the other hand, the lattice parameter of Nb_{ss} has not been reported systematically. Due to the wide compositional region of the Nb_{ss} phase (up to 20 mol% Al at high temperature), the lattice parameter of Nb_{ss} is expected to change widely depending on Al content. To determine the lattice parameter of Nb_{ss} in the wide range, XRD analysis and quantitative EPMA for Nb_{ss} were carried out. The results of EPMA are listed in Table 1.

Fig. 6 shows XRD patterns obtained for Nb, Nb–3Al, Nb–16Al and Nb–18Al. It is clearly seen that Nb and Nb–3Al are a Nb_{ss} single phase of A2, and that Nb–16Al and Nb–18Al are two phases of A2 and A15, as expected from Fig. 1. In both two-phase alloys, it is very difficult to identify all reflections from Nb_{ss} precisely, because a lot of peaks are overlapped between peaks of Nb_{ss} and Nb_3Al . In this study, four reflections from (211), (310), (321) and

Fig. 6. XRD patterns of Nb and Nb–Al alloys containing Nb solid solution (Nb_{ss}) investigated.

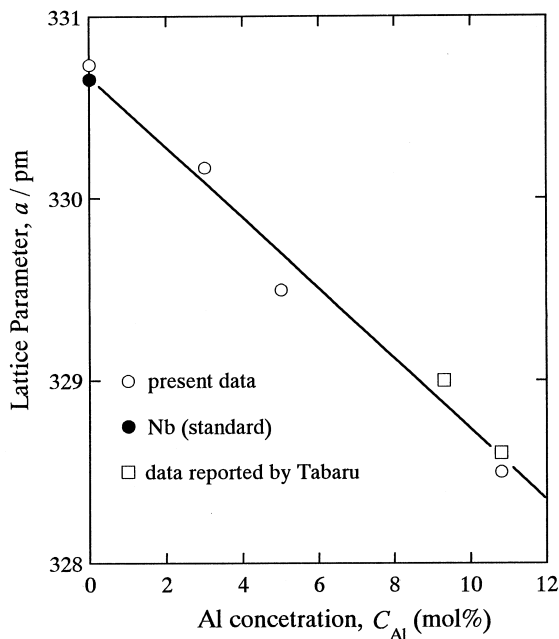


Fig. 7. Lattice parameter of Nb and Nb solid solution as a function of Al concentration. Data in the literature are added [14,15].

(400) of Nb_{ss} are employed for the precise lattice parameter determination. The results of lattice parameters as a function of Al concentration is shown in Fig. 7, where data in the literature are added [14,15]. The lattice parameter of pure Nb used in this study is measured to be 330.7 pm, which is in good agreement with that of standard Nb (330.66 pm) [14]. It is clear that the lattice parameter of Nb_{ss} decreases linearly with increasing Al content. Thus, it is concluded that the size of Al atoms in Nb_{ss} is smaller than that of Nb.

3.5. Effect of Al on hydrogen solubility and hydrogen diffusivity in Nb

As mentioned, the amount of hydrogen absorption in bulk Nb alloys is much reduced by adding Al. This reduction of hydrogen absorbed might be related to (1) the size of interstitial sites and/or (2) hydrogen diffusivity in Nb_{ss} . It is accepted that the lattice size of β -NbH as well as Nb_{ss} is reduced by increasing Al content. Consequently, the size of interstitial sites, i.e. tetragonal positions in β -NbH [10], decreases with increasing Al content. This leads to a reduction of hydrogen content in β -NbH. If the Al content of a Nb–Al alloy exceeds a critical amount, the alloy cannot absorb a sufficient amount of hydrogen for ordering. The long-range ordering of interstitial hydrogen atoms is in the nature of β -NbH [10]. This means that a Nb–Al alloy with hydrogen content below a critical value cannot transform into β -NbH.

The reduction of hydrogen absorption can also be explained if hydrogen diffusivity is assumed to be lowered

by adding Al, which leads to low hydrogen content after finite duration in the hydrogen environment. It should be noted again that it took about 4 h to obtain every hydrogen absorption and desorption curve in this study. The reduction of hydrogen diffusivity is explained from the standpoint of elastic and electronic interactions. Elastic strain field induced by substitutional atoms is known to strongly interact with interstitials, in this case, hydrogen [8]. Applying Vegard's law to the Al dependence of the lattice parameter in Fig. 7, the atomic radius of Al in Nb_{ss} is evaluated to be 133.0 pm. This value is 7.1% smaller than that of Nb (143.2 pm). This size mismatch generates a large elastic strain field in the Nb_{ss} lattice, which strongly interacts with hydrogen atoms in long range. This elastic field is suggested to reduce hydrogen diffusivity.

Assuming that Al atoms form a bcc crystal structure, the atomic radius of 'bcc' Al is calculated to be 139.2 pm under the constant atomic volume. The condition of constant atomic volume is generally a good approximation because transformation energy in solids is always very small compared to total energy. It is clear that the atomic radius of Al atoms in Nb_{ss} (133.0 pm) is smaller than that in 'bcc' Al (139.2 pm). In Nb_{ss} , a part of valence electrons around Al atoms are suggested to be taken by Nb atoms due to the electronegativity (E_N) difference (E_N is 1.5 for Al and 1.6 for Nb [16]). Also, hydrogen atoms exist as protons (H^+) in metals [17]. Therefore, Al atoms in Nb_{ss} have a strong repulsive force to H atoms (H^+) due to their positive ionic character. Al addition to Nb_{ss} is suggested to reduce hydrogen diffusivity remarkably due to such elastic and electronic interactions.

4. Summary

The effect of Al addition on the lattice parameter and the hydrogen absorption of various Nb–Al alloys were investigated using bulk specimens. The single phase alloys, Nb, Nb_{ss} and Nb_3Al , are not pulverized under the experimental conditions regardless of hydrogen absorption. Two-phase alloys are pulverized when a 'plateau' appears on the hydrogen absorption curves. The plateau corresponds to the rapid increase of the fresh surface by pulverization, not to hydride formation. Hydrogen absorption is also remarkably reduced by Al addition to Nb. The lattice parameter of Nb_{ss} is linearly reduced with increasing Al content. It is suggested that a hydride of β -NbH is formed in Nb and Al addition prevents the hydride formation. The atomic radius of Al atoms in Nb_{ss} is evaluated to be 133.0 pm, which is smaller than that of Nb atoms (143.2 pm) and that of 'bcc' Al calculated (139.2 pm). It is estimated that Al addition to Nb causes a lattice distortion and/or an ionic repulsive field to hydrogen (proton, H^+), both of which reduce hydrogen diffusivity in Nb_{ss} .

Acknowledgements

The present work was supported by the Grant-in-Aid for Science Research from the Ministry of Education, Science, Sports and Culture, Japan grant no. 07555509.

References

- [1] Y. Umakoshi, Bull. Japan Inst. Metals 30 (1991) 72.
- [2] S. Hanada, Proceedings of the 5th Symposium in High-performance Materials for Severe Environments, Industrial Science and Technology Frontier Program, R&D Institute of Metals and Composites for Future Industries, Tokyo, Japan, 1994, p. 95.
- [3] Y. Murayama, T. Kumagai, S. Hanada, in: I. Baker, R. Darolia, J.D. Whittenberger, M.H. Yoo (Eds.), High-temperature Ordered Intermetallic Alloys, Materials Research Society, Pittsburgh, PA, 1993, p. 95.
- [4] J.L. Jorda, R. Flükiger, J. Muller, J. Less-Common Met. 75 (1980) 227.
- [5] U.R. Kattner, in: T.B. Massalski, J.L. Murray, L.H. Bennett, H. Baker (Eds.), Binary Alloy Phase Diagrams, ASM, Materials Park, OH, 1986, p. 180.
- [6] S. Semboshi, T. Tabaru, H. Hosoda, S. Hanada, Intermetallics 6 (1998) 61.
- [7] S. Semboshi, H. Hosoda, S. Hanada, J. Jpn. Inst. Met. 61 (1997) 1132.
- [8] J. Völkl, G. Alefeld, in: G. Alefeld, J. Völkl (Eds.), Hydrogen in Metals I, Topics in Applied Physics, vol. 28, Springer-Verlag, Berlin, Germany, 1978, p. 321.
- [9] J.F. Smith, in: T.B. Massalski, J.L. Murray, L.H. Bennett, H. Baker (Eds.), Binary Alloy Phase Diagram, ASM, Metals Park, OH, 1983, p. 1271.
- [10] T. Schober, H. Wenzl, in: G. Alefeld, J. Völkl (Eds.), Hydrogen in Metals II, Topics in Applied Physics, vol. 29, Springer-Verlag, Berlin, Germany, 1978, p. 11.
- [11] L. Murugesu, K.T. Venkateswara Rao, R.O. Ritchie, Scripta Metall. Mater 29 (1993) 1107.
- [12] H. Hosoda, S. Hanada (to be published).
- [13] R.F. Decker, C.T. Sims, in: C.T. Sims, W.C. Hagel (Eds.), The Superalloys, John Wiley and Sons, NY, 1972, p. 31.
- [14] Kinzoku Data Book, 3rd ed.: Jpn. Inst. Met. (Eds.), Maruzen, Tokyo, Japan, 1993, p. 38.
- [15] T. Tabaru, Ph.D. Thesis, Tohoku University, 1997, p. 107.
- [16] L. Pauling, in: The Nature of Chemical Bond, 3rd ed., Cornell Univ. Press, New York, NY, 1960.
- [17] J. Friedel, Ber. Bunsenges. Physik. Chem. 76 (1972) 828.